Cell Death and Differentiation (2014) 21, 462–474

www.nature.com/cdd

The miR-106b ~ 25 cluster promotes bypass of doxorubicin-induced senescence and increase in motility and invasion by targeting the E-cadherin transcriptional activator EP300

Y Zhou[1,2,6], Y Hu[1,2,3,6], M Yang[1], P Jat[4], K Li[2], Y Lombardo[2], D Xiong[1], RC Coombes[2], S Raguz[5] and E Yagüe*[,2]

Resistance to chemotherapeutic treatment, which is indirectly responsible for many cancer deaths, is normally associated with an aggressive phenotype including increased cell motility and acquisition of invasive properties. Here we describe how breast cancer cells overcome doxorubicin-induced senescence and become drug resistant by overexpression of the microRNA (miR)-106b ~ 25 cluster. Although all three miRs in the cluster contribute to the generation of doxorubicin resistance, miR-25 is the major contributor to this phenotype. All three miRs in this cluster target EP300, a transcriptional activator of E-cadherin, resulting in cells acquiring a phenotype characteristic of cells undergoing epithelial-to-mesenchymal transition (EMT), including an increase in both cell motility and invasion, as well as the ability to proliferate after treatment with doxorubicin. These findings provide a novel drug resistance/EMT regulatory pathway controlled by the miR-106b ~ 25 cluster by targeting a transcriptional activator of E-cadherin.

Cell Death and Differentiation (2014) **21,** 462–474; doi:10.1038/cdd.2013.167; published online 22 November 2013

Chemotherapy is an important and in some cases the sole therapeutic option for most cancer patients. While the majority of cancers initially respond to chemotherapeutic drugs, acquired cross resistance to a variety of structurally and mechanistically unrelated drugs develops during treatment, leading to relapse and disease progression. Numerous mechanisms by which cancer cells become resistant have been described, including increased drug efflux,[1] dysregulation of cell death pathways,[2] activation of repair mechanisms of drug-induced DNA damage or the induction of drug-detoxification enzymes.[3] In addition, the acquisition of the epithelial–mesenchymal transition (EMT)-like phenotype of cancer cells and cancer stem cells (CSCs) also have critical roles in drug resistance.[4] Although key regulators of the tumorigenic process, such as p53 and pRb, have been found to control drug resistance before the full oncogenic transformation has taken place, how drug resistance arises is still unresolved.[5]

The effect of doxorubicin on cells, especially at the moderate-to-low concentrations likely to be found in the poorly vascularized, hypoxic regions of tumors,[6] typically leads to a senescent-like phenotype often termed therapy-induced senescence.[7] Following an initial arrest at G2, cells stop proliferating, upregulate senescence-associated (SA)-β-galactosidase activity, increase in size, and become polymorphic and polyploid, with a substantial fraction becoming multinucleated.[7,8] This phenotype, which resembles replicative and oncogene-induced senescence,[9] can also be triggered by other DNA-damaging drugs or γ-irradiation,[10] and is controlled by the p53-p21 axis,[11,12] pRb[13] and is dependent on telomere dysfunction.[14] Importantly, cells undergoing therapy-induced senescence can recover and resume proliferation,[10,15] although the mechanisms involved are not well understood.

MicroRNAs (miRs) are a class of 18- to 24-nucleotide single-stranded noncoding RNAs that function as negative regulators of gene expression by triggering translation repression through partial complementation to 3′-untranslated region (UTR) of target mRNAs.[16] MiRs have crucial roles in multiple biological processes and its expression is dysregulated in many cancers.[17,18] MiR genes are frequently located at fragile sites and cancer-associated genomic regions,[19] where they can function as oncogenes[20] or tumor suppressors.[21] Several reports indicate that miRs are also involved in

[1]State Key Laboratory of Experimental Hematology, Institute of Hematology and Blood Diseases Hospital, Chinese Academy of Medical Sciences and Peking Union Medical College, Tianjin, China; [2]Division of Cancer, Imperial College London, Hammersmith Hospital Campus, London, UK; [3]Department of Breast Cancer, China Tianjin Breast Cancer Prevention, Treatment and Research Center, Tianjin Medical University Cancer Institute and Hospital, Tianjin, China; [4]MRC Prion Unit, University College London, London, UK and [5]Institute of Clinical Sciences, Imperial College London, Hammersmith Hospital Campus, London, UK
*Corresponding author: E Yagüe, Division of Cancer, Imperial College London Faculty of Medicine, Hammersmith Hospital Campus, Du Cane Road, London W12 0NN, UK. Tel: +44 2075942802; Fax: +44 2083835830; E-mail: ernesto.yague@imperial.ac.uk
[6]Joint first authors.
Keywords: doxorubicin-induced senescence; EMT; cancer stem cells; E-cadherin; EP300
Abbreviations: ALDH, aldehyde dehydrogenase; CSC, cancer stem cell; EMT, epithelial–mesenchymal transition; ESF, primary human embryonic skin fibroblast; MCM7, minichromosome maintenance complex component 7; MD60, doxorubicin-resistant MTMEC; miR, microRNA; MTMEC, minimally transformed mammary epithelial cell; SA, senescence associated; UTR, untranslated region
Received 10.5.13; revised 19.10.13; accepted 22.10.13; Edited by S Kaufmann; published online 22.11.13

drug resistance.[22,23] However, the interplay between miRs, EMT, CSCs and drug resistance is not well characterized.

The miR-106b∼25 cluster, consisting of miR-106b, miR-93 and miR-25, is located in intron 13 of the minichromosome maintenance complex component 7 (*MCM7*) oncogene. It has been associated with tumor growth, cell survival and angiogenesis,[24,25] and may have an important proto-oncogenic role in cellular transformation and tumorigenesis by downregulation of several tumor suppressors such as p21, E2F1, Bim and PTEN.[26–28]

In this report, we show that the miR-106b∼25 cluster negatively regulates the histone acetyltransferase EP300, a transcriptional activator of E-cadherin. This leads to doxorubicin-induced senescence bypass, activation of the EMT process, increase in the ability of cell migration and invasion, and consequently the induction of an EMT-associated drug resistance phenotype.

Results

The miR-106b∼25 cluster is upregulated in doxorubicin-resistant cells. Doxorubicin is one of the main therapeutics to treat breast cancer. We used minimally transformed mammary epithelial cells (MTMECs) that represent a cellular model of breast cancer in which transformation of primary mammary epithelial cells has been achieved by selective manipulation of key molecules or pathways involved in tumorigenesis,[29] to derive doxorubicin-resistant cells (MD60). These drug-resistant cells were generated using a regime of doxorubicin pulses followed by drug-free periods, as suggested to mimic the administration of chemotherapy to cancer patients.[30] Although other studies have used much higher doxorubicin concentrations,[31] in the clinic, Adriamycin typically reaches plasma concentrations of ∼600 ng/ml during the first hour after intravenous administration, which is reduced to ∼40–50 ng/ml from 8 h onward.[32] In addition, owing to their abnormal vasculature, many regions in a tumor are poorly vascularized, hypoxic and with poor distribution of doxorubicin,[6] so doxorubicin concentrations in the low ng/ml range have an important physiological significance. The doxorubicin concentration used was determined empirically to induce a typical senescent phenotype (Figures 1a and b) and was within the range used previously in the generation of doxorubicin-resistant cells from primary human embryonic skin fibroblasts (ESFs) that are able to bypass drug-induced senescence.[5] MD60 cells did not show hallmarks of senescent cells, in that they did not show activation of acidic β-galactosidase, and were able to resume proliferation after doxorubicin treatment (Figures 1a and b). In order to identify novel modulator of molecules involved in the doxorubicin resistance phenotype, we screened sensitive MTMECs and their resistant derivative (MD60 cells) for differentially

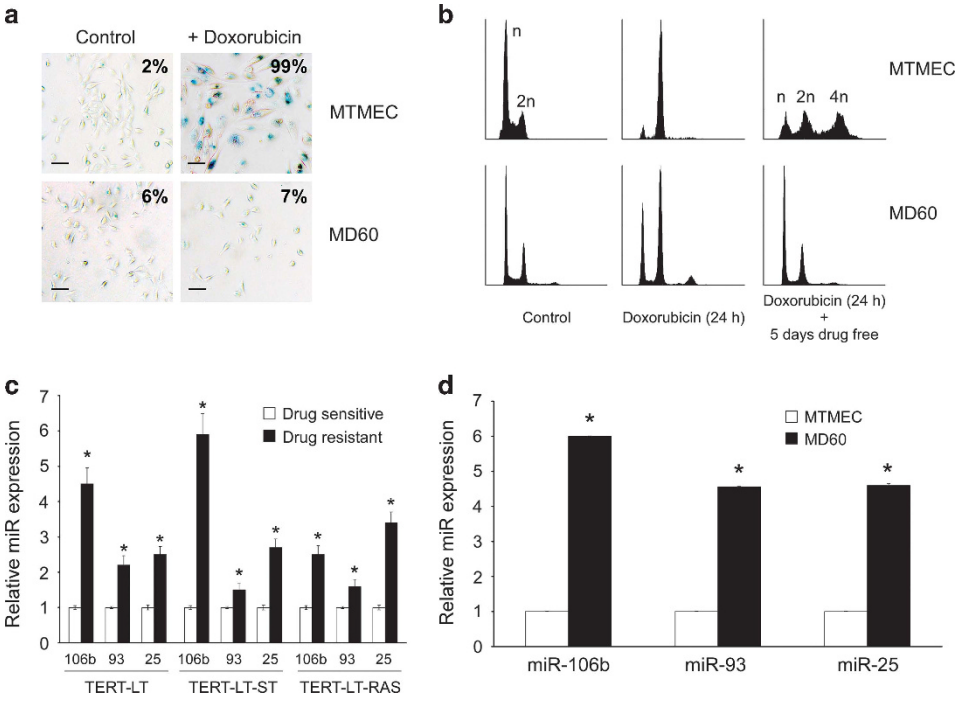

Figure 1 The miR-106b∼25 cluster is upregulated in drug-resistant cells. (**a**) Doxorubicin-resistant cells (MD60) bypass drug-induced senescence. SA-β-galactosidase staining after treatment with 60 ng/ml doxorubicin for 24 h followed by 5 days drug-free culture. Percentage of senescent cells is indicated after monitoring at least six fields of view (typical variation approximately 10%). Bar represents 30 μm. (**b**) Cell cycle profiles by flow cytometry after propidium iodide staining. Both MTMEC and MD60 cells showed an initial G2 arrest after exposure to doxorubicin for 24 h (middle panels), but MTMEC cells did not proliferate any further, with some cells showing a tetraploid DNA content (upper right panel), whereas drug-resistant MD60 cells did resume proliferation and showed a cell cycle profile (lower right panel) similar to that of untreated cells (left panels). X axis represents DNA content and y axis cell number. (**c** and **d**) Expression of miRs 106b, 93 and 25 was determined by reverse transcription and real-time PCR using TaqMan probes and was normalized to the expression of *U6* RNA. Expression was determined in previously described models from pre-tumorigenic ESFs[5] (**c**) and (**d**) drug-resistant derivatives of MTMEC cells (**d**). Data represent the average ± S.D. of three different experiments (*$P<0.05$). In all cases, expression data show fold upregulation in drug-resistant cells with respect to drug-sensitive cells

expressed miRNAs using commercially available arrays. Only four miRs were differentially expressed more than twofold between these cells, the miRs comprising the miR-106b~25 cluster and miR-34a (Supplementary Figure S1).

Both ESF- and MTMEC-derived resistant cells showed upregulation of the miR-106b~25 cluster (Figures 1c and d). To determine whether the miR-106b~25 cluster might be directly involved in the generation of doxorubicin resistance, we cloned the human genomic region harboring the miR-106b~25 cluster in a lentiviral vector and generated stable transfectants of MTMEC cells (MTMEC-miR-106b~25; Figure 2a). Despite being expressed from the same vector, miR-25 levels were higher than those of miR-93 and twice as those of miR-106b, probably reflecting different miR turnover rates. Overexpression of the miR-106b~25 cluster allowed cells to bypass doxorubicin-induced senescence and increased the capacity of MTMEC cells to generate doxorubicin-resistant cells (Figures 2b–d). Equally, when we downregulated miR-106b~25 cluster expression in drug-resistant MTMEC cells, MD60, and treated them with doxorubicin, their proliferation in the presence of doxorubicin was reduced (Figures 2e–g), indicating that the cells had become more sensitive to the drug. Importantly, MD60 cells were resistant to γ-irradiation (Supplementary Figure S2A) and MTMEC-miR-106b~25 cells bypassed γ-irradiation-induced senescence and generated more resistant clones than control cells (Supplementary Figure S2B).

Members of the miR-106b~25 cluster have been shown to promote cell cycle progression[25] and tumor growth,[24] however, we did not detect any difference in cell growth under drug-free conditions (Supplementary Figure S3). Thus, in the absence of doxorubicin, the miR-106b~25 cluster does not affect cell proliferation of MTMEC cells.

PTEN-dependent miR-106b~25 oncongenic activity requires the cooperation of the *MCM7* host gene.[26] As overexpression of *MCM7* has also been identified in a number of malignancies,[33] drug-resistant KB-v1cells[34] and MD60 cells (Supplementary Figure S4A), we also asked whether *MCM7* could, at least partially, be responsible for the generation of doxorubicin resistance in mammary epithelial cells. For this, we overexpressed the coding region of *MCM7* in a lentiviral vector and performed clonogenic assays after doxorubicin treatment. Although the experimental expression of the transgene in MTMEC cells resulted in an approximately 10-fold upregulation of that found in MD60 cells (Supplementary Figure S4B), MTMEC-MCM7 cells did not increase the number of doxorubicin-resistant clones generated compared with MTMEC control cells transfected with the empty vector (Supplementary Figures S4C and D). Thus, the generation of drug resistance by the miR-106b~25 cluster is *MCM7* independent.

Therefore, the overexpression of the miR-106b~25 cluster allows breast cancer cells to bypass doxorubicin and radiation-induced senescence and promotes the generation of therapy resistance.

MiR-25 is a major contributor in the development of doxorubicin resistance. To ascertain the contribution of each miR to the generation of doxorubicin resistance, we expressed each individual pre-miR in a lentiviral vector, transfect them into MTMEC cells (Figure 3a) and performed long-term clonogenic drug resistance assays. Indeed, cells overexpressing miR-25 generated a higher number of doxorubicin-resistant clones than those expressing either miR-106b or miR-93 (Figures 3b and c). However, cells expressing either of these two last miRs generated more clones than control cells. This was confirmed and quantified by EdU incorporation cell proliferation assays (Figures 3d and e). Interestingly, when the whole cluster was expressed in MTMEC cells, miR-25 levels were higher than those of miR-93 and miR-106b (Figure 2a). Thus, although the three miRs in the miR-106b~25 cluster are able to generate doxorubicin resistance, miR-25 is the major contributor to this phenotype.

The individual miRs in the miR-106b~25 cluster have proto-oncogenic activity in breast cancer cells. Drug-resistant cells have been proposed to arise from the selection of a small population of pre-existing cells with stem cell-like properties.[35] We asked then whether the miR-106b~25 cluster would have an effect on the stemness of MTMEC cells. As these cells are intrinsically CD44 ^{high}/CD24^{low} because of oncogenic RAS expression[36] (Supplementary Figure S5), we used aldehyde dehydrogenase (ALDH) detection as a surrogate for stemness.[37] Emergence of doxorubicin resistance was indeed accompanied by an increase in the percentage of ALDH-positive cells (30% of MD60 cells; Figure 4a).

The miR-106b~25 cluster has been reported to be proto-oncogenic in prostate cells,[26] and miR-93 in an astrocytoma cell line.[24] We asked whether the whole miR-106b~25 cluster, or the individual miRs, had a proto-oncogenic effect on MTMECs. Indeed, expression of the miR-106b~25 cluster in MTMEC cells nearly doubled the formation of clones growing in soft agar when compared with control cells (MTMEC-ev). In addition, blocking the effect of miRs using ZIP anti-miR interference (MTMEC-ZIP- miR-106b~25 cells) restored clone numbers similar to those found in MTMEC-ev cells (Figure 4b). Although miR-25 has a dominant role of in the development of drug resistance (Figure 3), all miRs in the miR-106b~25 cluster contributed equally to the enhancement of anchorage independence in MTMEC cells (Figure 4c).

Drug-resistant cells typically exhibit a more aggressive phenotype, clinically characterized by metastatic invasion and formation of new secondary tumors.[2,38] As the miR-106b~25 cluster enhances the tumorigenic potential of MTMEC cells, we asked whether the same would apply to doxorubicin-resistant MD60 cells (with upregulated miR-106b~25 cluster expression). Indeed this was the case, as MD60 cells formed a higher number of clones in soft agar than MTMEC cells, which decreased when ZIP anti-miR interference was used (MD60-ZIP- miR-106b~25 cells; Figure 4b).

Thus, to summarize, the three miRs in the miR-106b~25 cluster enhance the oncogenic potential of tumorigenic mammary epithelial cells.

The miR-106b~25 cluster regulates EMT by down-regulation of E-cadherin via targeting its transcriptional activator EP300. Wound-healing assays were performed to determine whether overexpression of the miR-106b~25

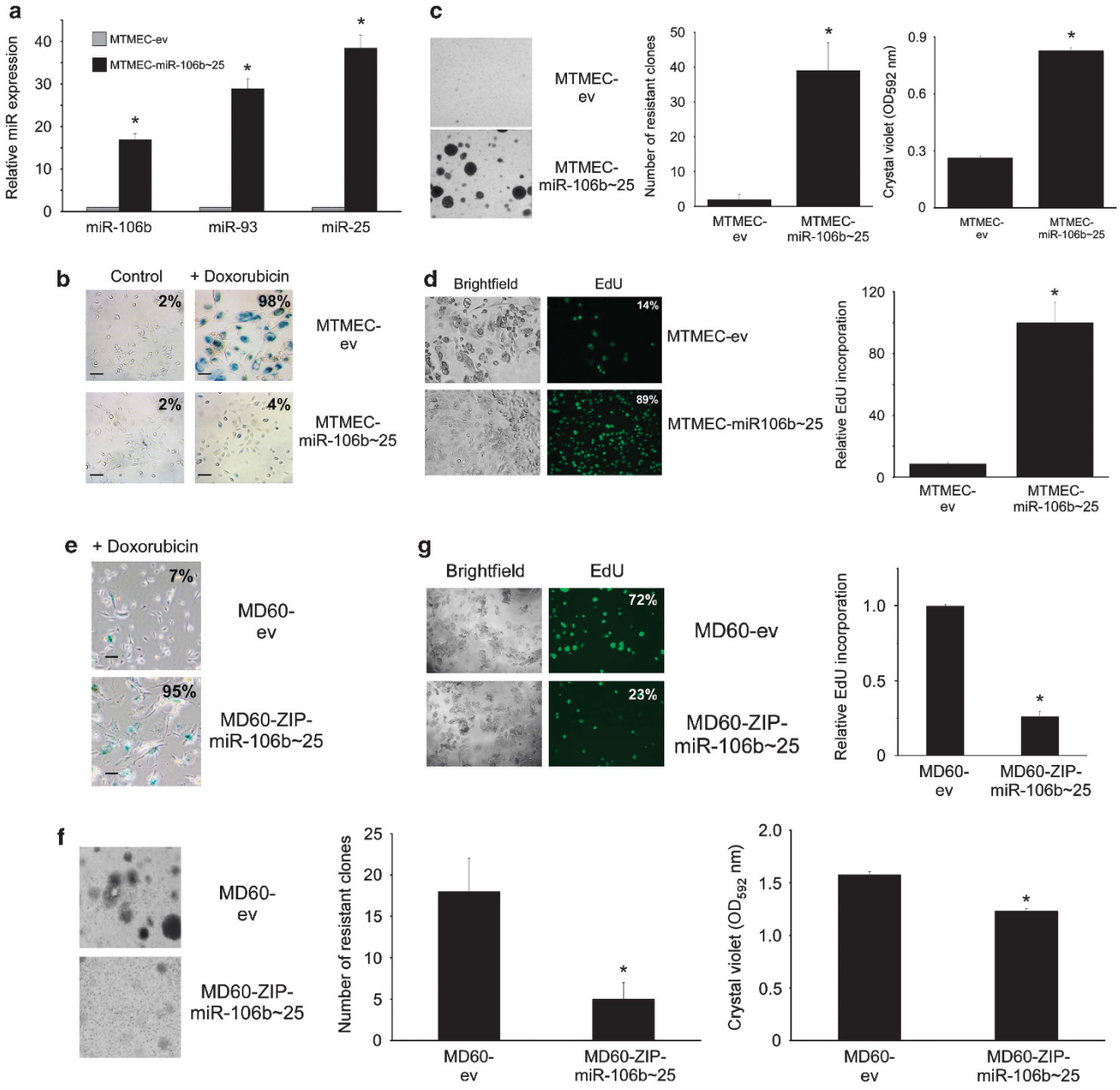

Figure 2 The miR-106b ~ 25 cluster allows cells to bypass doxorubicin-induced senescence and to generate drug resistance. (**a**–**d**) MTMEC cells were stably infected with a lentiviral vector expressing the miR-106b ~ 25 cluster genomic sequence (intron 13 of MCM7). (**a**) MiR expression was determined by reverse transcription and real-time PCR using TaqMan probes and was normalized to *U6* RNA. (**b**) Bypass of doxorubicin-induced senescence in cells overexpressing the miR-106b ~ 25 cluster. Cells were treated with 60 ng/ml doxorubicin for 24 h and stained for SA-β-galactosidase 3 weeks after. Percentage of senescent cells is indicated after monitoring at least six fields of view (typical variation approximately 10%). Bar represents 30 μm. (**c**) Cells overexpressing the miR-106b ~ 25 cluster are able to generate doxorubicin-resistant clones. Cells were treated for 24 h with 60 ng/ml doxorubicin and drug-resistant clones were stained with crystal violet after 3 weeks (left panel), counted (middle panel) and crystal violet was solubilized (right panel). (**d**) MiR-106b ~ 25 overexpressing cells were able to proliferate after doxorubicin challenge. Cells were treated with doxorubicin as above and 3 weeks later, trypsinized and seeded (10 000 cells per well in a 96-well plate). EdU was added to the medium and left for 18 h to allow its incorporation into newly synthesized DNA. Cells were monitored using both brightfield and fluorescence and the percentage of cells incorporating EdU determined after examination of at least three fields of view (left panels). EdU incorporation was determined in the well using a fluorimeter (right panel). (**e**–**g**) Downregulation of miR-106b ~ 25 cluster expression in drug-resistant MD60 cells restores drug sensitivity. MD60 cells were stably infected with a lentiviral ZIP construct to downregulate endogenous miR-106b ~ 25 cluster expressions and were treated with 240 ng/ml doxorubicin for 24 h and then were left drug free for 3 weeks to enable the generation of doxorubicin-resistant clones. (**e**) SA-β-galactosidase. Percentage of senescent cells is indicated after monitoring at least six fields of view (typical variation approximately 10%). Bar represents 30 μm. (**f**) Cultures were stained with crystal violet (left panel), the number of drug-resistant clones counted (middle panel) and crystal violet solubilized and the optical density determined (right panel). (**g**) EdU incorporation as in **d**. Numerical data represent the average ± S.D. of at least three different experiments ($^*P < 0.05$). Pictorial data were repeated at least in triplicate and a representative picture is shown

cluster had an impact on cell migration. Indeed, cells overexpressing the miR-106b ~ 25 cluster, or its individual miRs, were more motile and closed the wound faster than their control counterparts. Of the individual miRs, miR-106b had a predominant role in this assay (Figure 5a). To assess quantitatively migration and invasion, two key properties of

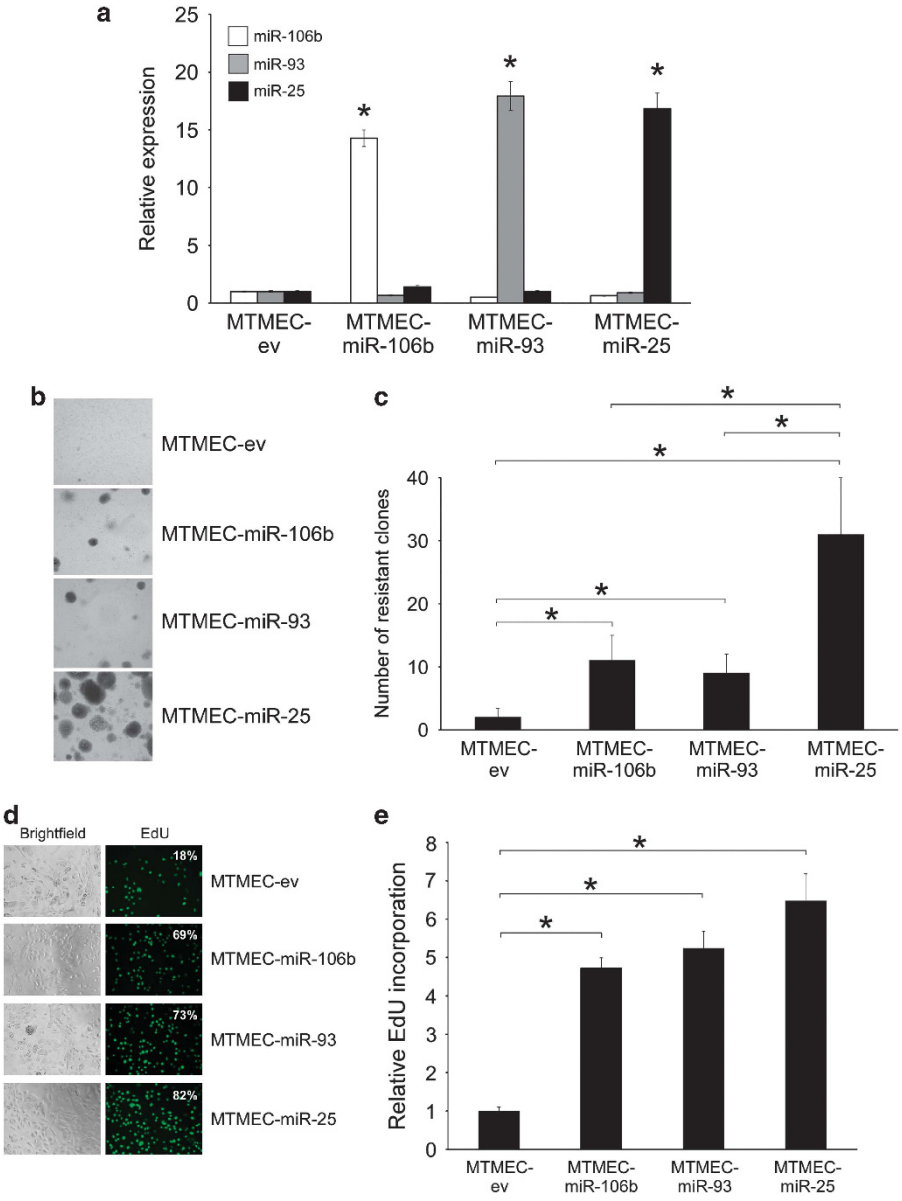

Figure 3 MiR-25 is a major contributor to doxorubicin resistance. MTMEC cells were transfected with lentiviral vectors harboring genomic sequences of individual miRs to generate MTMEC-miR-106b, MTMEC-miR-93 and MTMEC-miR-25 cells (cells transfected with the empty vector, MTMEC-ev, were used as control). (**a**) Expression of miRs was determined by reverse transcription and real-time PCR using TaqMan probes and was normalized to the expression of *U6* RNA. Cells were treated for 24 h with 60 ng/ml doxorubicin and (**b**) drug-resistant clones were stained with crystal violet after 3 weeks and (**c**) counted. (**d**) Percentage of cells incorporating EdU by fluorescence microscopy. (**e**) EdU incorporation determined by fluorescence detection. Numerical data represent the average of three independent experiments ± S.D. (*$P<0.05$). Pictorial data show a representative of at least three independent replicates

cells undergoing EMT, we then used transwells with or without Matrigel in order to measure invasion and migration, respectively. Drug-resistant MD60 cells showed an increase in their motility and invasion when compared with naive MTMEC cells (Figures 5b and c). That this phenotype was due to the miR-106b∼25 cluster expression was confirmed when the cluster expression was knocked-down in MD60-ZIP-miR-106b∼25 cells (Figure 2f), reverting to migration and invasion levels as of MTMEC cells (Figures 5b and c). In addition, overexpression of the miR-106b∼25 cluster, or the individual miRs, in MTMEC cells showed an increase in both migration and invasion (Figures 5b and c), although miR-106b and miR-25 contributed more to the motility of cells in the transwell assay (Figure 5b).

The miR-106b∼25 cluster has recently been reported to induce EMT via targeting Smad7.[28] However, the observed increased in motility and invasion was not due to down-regulation of *SMAD7,* neither in MTMEC cells overexpressing the miR-106b∼25 cluster nor in MD60 cells (Supplementary Figure S6). Moreover, *SIX1*, which has been reported to be a trans-activator of miR-106b∼25 cluster expression in MCF-7 cells[28] was found to be downregulated in these cells (Supplementary Figure S6). We also interrogated the expression levels of a panel of genes responsive to TGF-β signalling

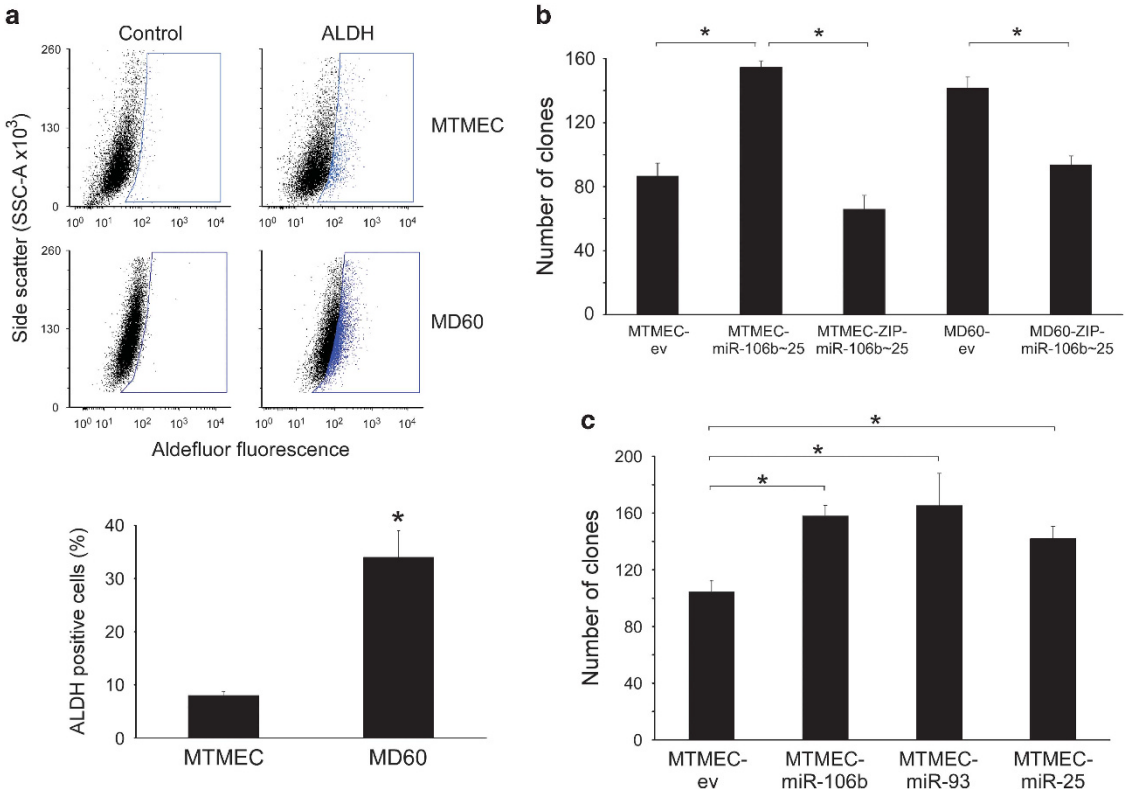

Figure 4 The individual miRs in the miR-106b~25 cluster have proto-oncogenic activity in breast cancer cells. (**a**) Doxorubicin resistance is accompanied by an increase in the percentage of ALDH-positive cells. Drug-sensitive MTMEC cells were used to generate drug-resistant derivatives able to proliferate after 24-h exposures to 60 ng/ml (MD60) of doxorubicin. For ALDH activity, cells were treated with Aldefluor alone (*ALDH*) or in the presence of the ALDH inhibitor diethylaminobenzaldehyde (*Control*) and then analyzed by flow cytometry. The blue gate was set up with the control cells to include no $>1\%$ of the population and was used to determine the percentage of ALDH-positive cells in the absence of inhibitor. Plots shown are representative of at least three independent experiments. (**b** and **c**) The individual miRs in the miR-106b~25 cluster have proto-oncogenic activity in breast cancer cells. Anchorage independence was determined by the formation of clones in soft agar after 4 weeks. (**b**) MTMEC cells transfected with a lentiviral vector expressing the miR-106b~25 cluster (MTMEC-miR-106b~25). A ZIP anti-miR lentiviral vector was used to knock-down miR-106b~25 cluster expression in both MTMEC and drug-resistant MD60 cells. (**c**) Expression of individual miRs in MTMEC cells led to the formation of similar number of anchorage-independent clones. In all cases, cells transfected with empty vectors (*ev*) were used as controls. Data represent the average ± S.D. of at least three independent experiments ($^*P<0.05$)

both upon experimental overexpression of the miR-106b~25 cluster and in drug-resistant MD60 cells. Only 4 out of 16 genes were upregulated (more than twofold) in MTMEC cells overexpressing the miR-106b~25 cluster. Equally, only two genes were upregulated (more than twofold) in MD60 cells, and these were different from those found in MTMEC-miR-106b~25 cells (Supplementary Figure S7). Thus, although we cannot rule out a slight increase in certain TGF-β downstream targets upon miR-106b~25 cluster expression, the clear lack of correlation between *SIX1/SMAD7* and miR-106b~25 levels suggests that activation of migration and invasion by the miR-106b~25 cluster in MTMECs is *SIX1/SMAD7*/TGF-β independent.

Bioinformatic analysis to predict targets of the miR-106b~25 cluster[39] identified individual single sites for both mir-106b/93 and mir-25 in the 3′-UTR of *EP300.* As EP300 has been identified as a positive regulator of E-cadherin (*CDH1*) gene expression,[40] we hypothesized that a negative correlation should exist between the miR-106b~25 cluster and EP300 expression. Indeed, drug-resistant MD60 cells, which overexpress the miR-106b~25 cluster (Figure 1d), showed reduced *EP300* and *CDH1*, but increased *VIM* (encoding vimentin, a mesenchymal intermediate filament protein activated during EMT[4]) mRNA levels (Figure 6a). When the cluster expression was knocked-down in MD60-ZIP-miR-106b~25 cells leading to a decrease in migration and invasion (Figures 5b and c), expression of both *EP300* and *CDH1* mRNAs increased, and, as expected, *VIM* mRNA decreased (Figure 6b). In all cells, western blot analyses showed that downregulation of EP300 did associate with downregulation of its downstream target, E-cadherin, and upregulation of vimentin (Figure 6c). Although bioinformatic analysis of miR targets[39] predicted binding sites for miR-106b in the 3′-UTR of other *CDH1* transcriptional activators, *FOXA1* and *RUNX1*, these mRNAs were only marginally down-regulated when the miR-106b~25 cluster was overexpressed (Supplementary Figure S8). To experimentally confirm that *EP300* mRNA was a target of the miR-106b~25 cluster, we used a luciferase reporter with the 3′-UTR of *EP300* and transiently transfected either control or cells overexpressing the cluster or individual miRs. In all cases, luciferase expression from the plasmid containing the *EP300* 3′-UTR was lower in cells overexpressing both the miR-106b~25 cluster and its individual miRs (Figure 6d). Moreover, when a

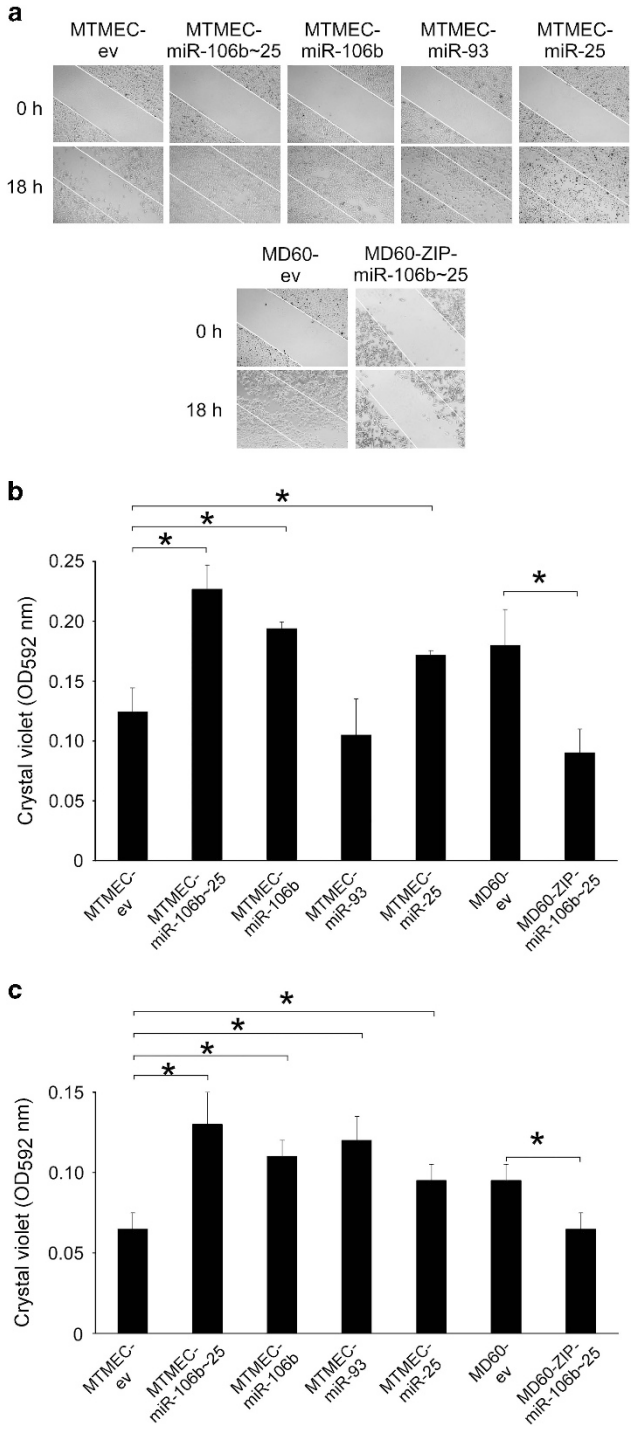

Figure 5 The miR-106b∼25 cluster regulates migration and invasion. Motility was monitored by the wound-healing assay (**a**) and quantified using trans-well assays (**b**), whereas invasion was quantified in the same way but using Matrigel-coated trans-well chambers (**c**). (**a**) Wounds were inflicted with a needle tip on confluent layer of cells (top panels) and monitored by microscopy 18 h later (bottom panels). The white lines define the areas lacking cells at the beginning of the experiment. (**b** and **c**) After 72 h, cells in the transwell were stained with crystal violet (upper panels) and then the dye was solubilized and quantified at 592 nm. Numerical data represent the average ± S.D. of at least three experiments (*$P<0.05$). Pictorial data show a representative of at least two replicates

mutation was introduced in the *EP300* 3′-UTR to abrogate either binding of miR-25 or miR-106b/93, the reduction of luciferase expression was cancelled (Figure 6e; Supplementary Figure S9).

Next, we asked whether the experimental downregulation of EP300, or E-cadherin, could reproduce the phenotype obtained by the upregulation of the mir-106b∼25 cluster. For this we generated stably transfected MTMEC cells expressing small hairpins to knock-down these mRNAs by RNA interference, thus generating MTMEC-shEP300 and MTMEC-shCDH1 cells (Figure 7a). These cells were more motile and invasive than the corresponding cells transfected with an empty vector and used as controls (Figure 7b). In addition, knock-down of either *EP300* or *CDH1* resulted in the bypass of doxorubicin-induced senescence and proliferation of doxorubicin-resistant clones (Figures 7c, d and e) and rendered cells more tumorigenic (Figure 7f). To corroborate these results, we used the same hairpins to transfect MCF-7 cells and thus generate MCF7-shEP300 and MCF7-shCDH1 cells (Figure 8a). These cells bypassed doxorubicin-induced senescence (Figure 8b) and generated doxorubicin-resistant clones (Figure 8c), although these phenotypes were more robust in MCF7-shEP300 than in MCF7-shCDH1 cells. Experimental downregulation of EP300 and E-cadherin led, as expected, to an increase in both motility and invasion (Figures 8d and e).

Thus, the miR-106b∼25 cluster targets *EP300* leading to downregulation of E-cadherin, bypass of doxorubicin- and irradiation-induced senescence, activation of EMT and generation of therapy resistance in breast cancer cells.

Discussion

During EMT, epithelial cells disrupt their cell–cell junctions and lose apico-basolateral polarity, resulting in the formation of migratory mesenchymal cells with invasive properties. Here we describe a novel regulatory axis controlling EMT, which is governed by the miR-106b∼25 cluster downregulating the E-cadherin transcriptional activator EP300. Importantly, cells overexpressing the miR-106b∼25 cluster, or in which either EP300 or E-cadherin has been downregulated, not only gain motility and invasive properties but are also able to generate drug-resistant derivatives, an additional characteristic of cells which have undergone an EMT. We show that DNA-damaging agents such as doxorubicin or γ-irradiation induce a senescent phenotype similar to the well-studied replicative- and oncogene-induced senescence, with activation of SA-β-galactosidase, cell morphological changes and proliferation arrest. The new regulators of the pathway described here, miR-106b∼25 cluster and EP300, when overexpressed, either experimentally or after drug selection, endow cells with the capacity to bypass the senescent phenotype. In addition, reporter assays indicate that all three miRs in the miR-106b∼25 cluster bind the 3′-UTR of *EP300* mRNA and contribute to doxorubicin-induced senescence bypass and generation of drug resistance, although miR-25 has a predominant role.

EMT inducers, such as TGF-β or receptor tyrosine kinase ligands, trigger changes in gene expression by complex signalling networks. As a consequence, well-studied transcriptional repressors such as those belonging to the Snail

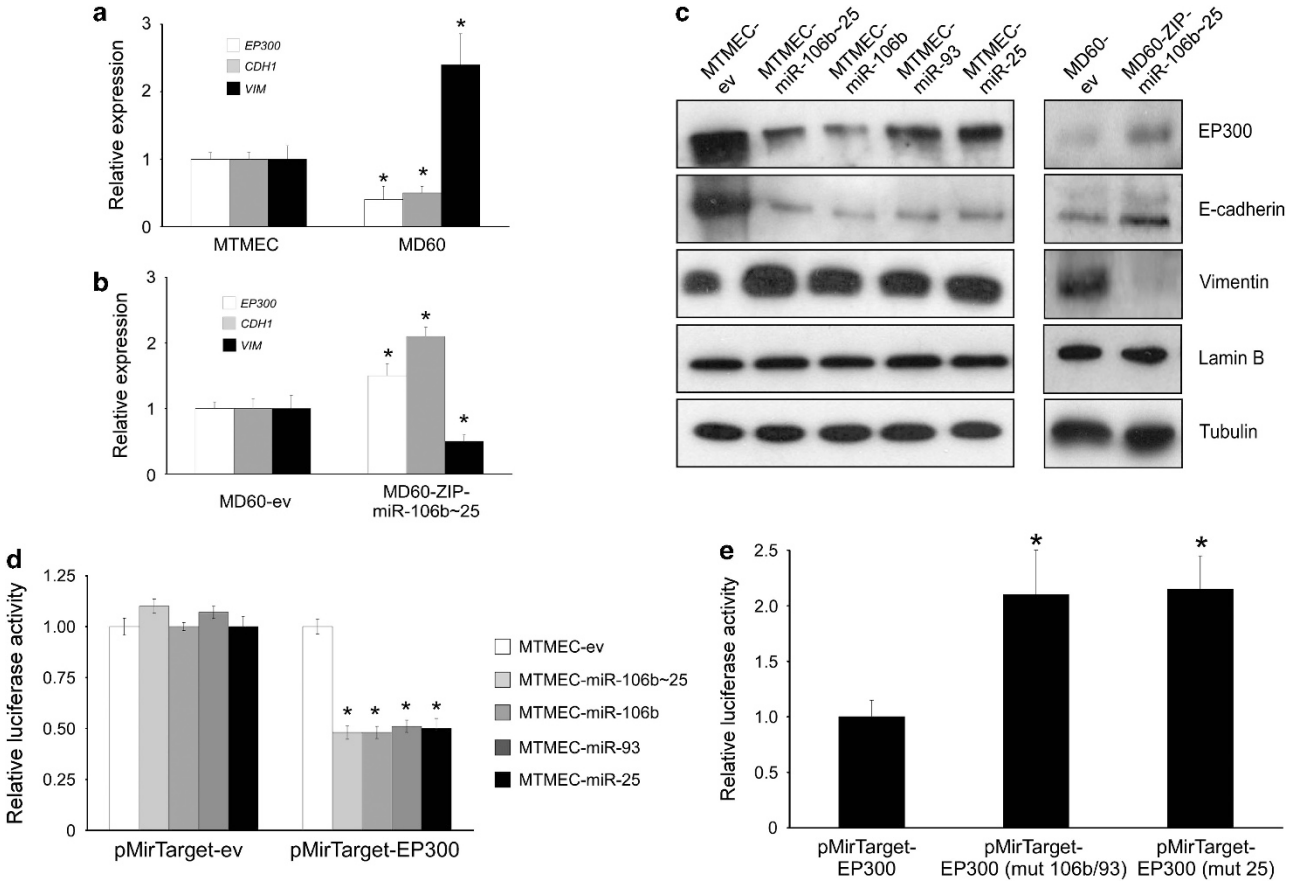

Figure 6 The mir-106b ~ 25 cluster targets the E-cadherin transcriptional activator EP300. (**a**–**c**) Expression of the miR-106b ~ 25 cluster, or its individual miRs, leads to down-regulation of EP300, a transcriptional activator of E-cadherin expression. (**a**) Expression analysis by reverse transcription and real-time PCR normalized to the expression of *RPS14* mRNA in doxorubicin-resistant cells. In drug-resistant MD60 cells, which over-express mir-106b ~ 25 cluster, both *EP300* and *CDH1* mRNAs are down-regulated, whereas *VIM* mRNA is up-regulated. (**b**) Rescue phenotype in cells stably transfected with a lentiviral ZIP construct to down-regulate endogenous miR-106b ~ 25 cluster expression. (**c**) Western blot showing down-regulation of *EP300* and E-cadherin and up-regulation of vimentin in cells over-expressing the miR-106b ~ 25 cluster, or its individual miRs. Both lamin B and tubulin were used as loading controls. (**d**) The miR-106b ~ 25 cluster targets EP300. Normalized firefly luciferase activity from the reporter with the *EP300* 3′-UTR (*pMirTarget-EP300*) or the empty vector (*pMirTarget-ev*) after transient transfection. In all cases cells were co-transfected with a *Renilla* luciferase expression vector to normalize for transfection efficiency. Expression of each construct was normalized to that of MTMEC cells. (**e**) The putative miR target sequence in *EP300* 3′-UTR was mutated to abrogate miR-106b/93 (*pMirTarget-EP300* (*mut 106b/93*)) or miR-25 binding (*pMirTarget-EP300 (mut 25)*) and used to transiently transfect MTMEC-miR-106b ~ 25 cells as in G. Numerical data show the average ± SD of at least three experiments (*$P < 0.05$) and the immunoblot shows a representative of at least three replicates

family (Snail, Slug), the two-handed zinc factors ZEB1 and ZEB2, as well as the bHLH factors Twist and E47, down-regulate E-cadherin expression leading to adherens junction breakdown, loss of cell polarity, increased motility and gain in the expression of mesenchymal markers, such as vimentin and N-cadherin, as well as increased activity of matrix metalloproteinases associated with an invasive phenotype.[41,42] On the other hand, the role of transcriptional activators of E-cadherin in the EMT context have not been addressed. In addition to EP300, FOXA1/2 and RUNX1 have been shown to bind the E-cadherin gene promoter and activate its transcription.[40] EP300 functions as histone acetyltransferase that regulates transcription via chromatin remodelling and acetylates all four core histones in nucleosomes. Although chromosomal translocations involving the *EP300* locus are rare in cancer, loss of heterozygosity has been described in colon, breast and ovarian carcinomas, suggesting a tumor-suppressor role.[43] In addition, somatic mutations in *EP300* have been identified in several malignancies.[44] Importantly, EP300-deficient colon carcinoma cells show phenotypic changes characteristic of EMT,[45] in line with the results reported here.

The involvement of miRs in drug resistance, CSCs (cells originated from adult stem cells, which have acquired tumorigenic properties and drive tumor growth and progression because of their unlimited proliferative potential), and EMT is now well established. For instance, ZEB1 and ZEB2 are direct targets of miR-200 and miR-205, two miRs triggering EMT,[46] miR-9 regulates E-cadherin and cancer metastasis,[47] miR-221/222 confer tamoxifen resistance by targeting p27,[48] and miR-214 regulares ovarian cancer cell stemness.[49] Several roles have previously been reported for the miR-106b ~ 25 cluster, such as regulation of transformation by inactivation of PTEN,[26] regulation of cell cycle progression by targeting p21[25] or regulation of apoptosis by targeting Bim.[27] Although in breast cancer MCF-7 cells, the

miR-106b~25 cluster has been shown to target Smad7, activate TGF-β signalling and induce EMT,[28] in MTMECs used in this study EMT induction/drug resistance occurs via targeting EP300. In the clinical setting, the miR-106b~25 cluster is associated with early prostate cancer recurrence[50] and the coordinated expression of its three miRs is associated with aggressive basal-like, ER-negative, grade 3 breast cancers.[51]

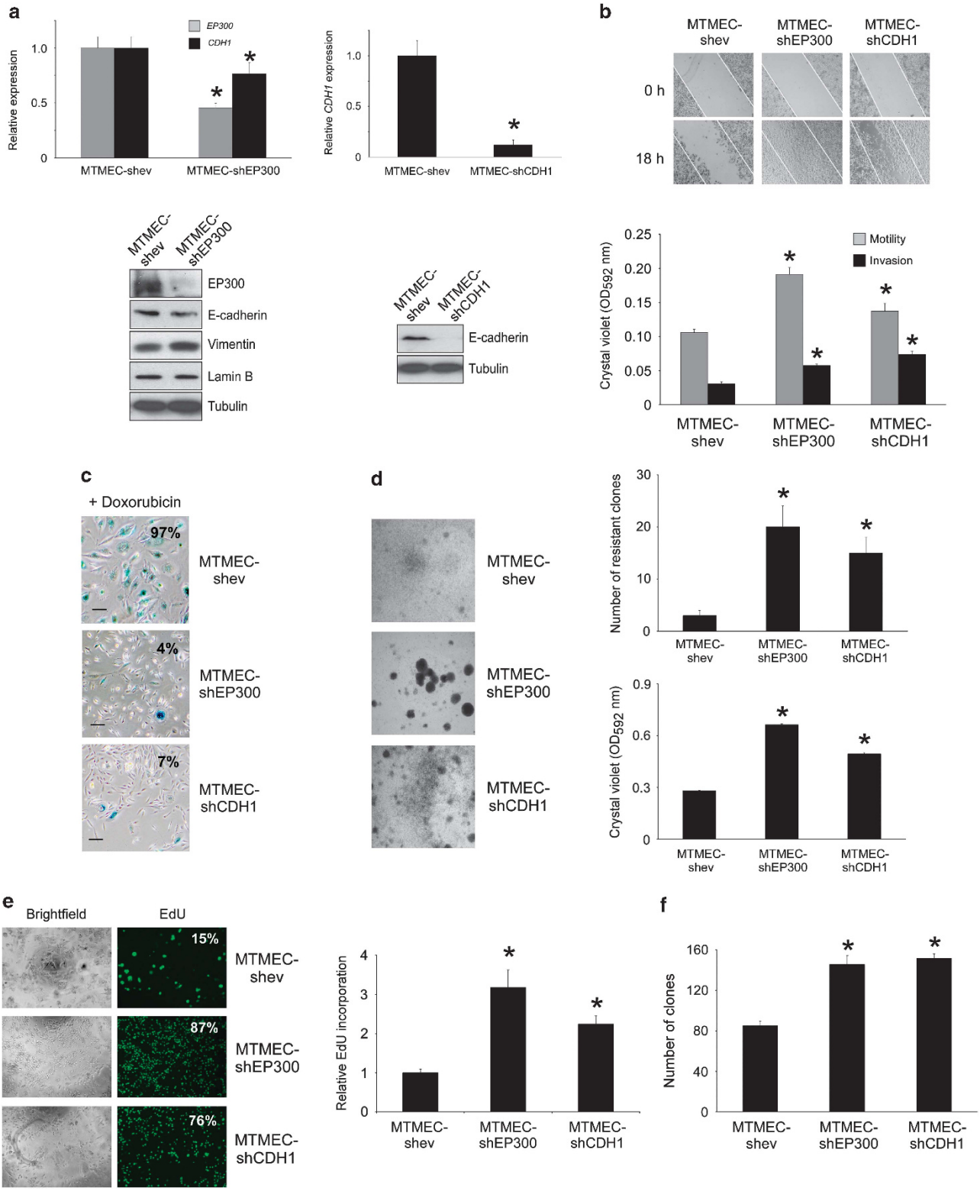

Downregulation of the hundreds of potential targets of a particular miR is frequently cell-type dependent. Here we show that the independent experimental downregulation of EP300 by RNA interference in two different cell models of breast cancer confirms that EP300 governs the EMT process by targeting E-cadherin gene expression. However, we cannot rule out that other miR-106b ~ 25 targets might contribute to the EMT/drug-resistant phenotype. Equally, as EP300 is a transcriptional activator, we cannot exclude the possibility that the expression of other target genes, in addition to *CDH1*, is reduced in EP300-downregulated cells. However, knock down of E-cadherin by RNA interference leads to bypass of doxorubicin-induced senescence and to the emergence of drug-resistant cells that are also more motile and invasive. This is in agreement with other reports in which loss of E-cadherin leads to EMT, invasiveness, anoikis resistance and angiogenesis.[52,53]

How drug resistance arises and what are the ultimate controllers of the process is still unsolved. Work done with cellular models of tumorigenesis has indicated that the same checkpoints altered during oncogenesis, such as inactivation of p53, are also the necessary and sufficient processes for the generation of drug resistance, even at the pre-tumorigenic stage.[5] In addition, some of the markers associated with CSCs such as ABCG2, have been shown to protect them from chemotherapeutic agents.[54] CSCs may then have a critical role in drug resistance as chemotherapy is capable of eliminating the differentiated cells forming the bulk of a tumor, while leaving intact CSCs able to repopulate and self-renew.[55] Our work indicates that drug-resistant mammary epithelial cells show an increase in ALDH-positive cells, a marker of CSC, suggesting that an increase in stemness accompanies the drug selection process. Importantly, anchorage-independent growth is enhanced in both drug-resistant cells and naive cells experimentally overexpressing the miR-106b ~ 25 cluster. Individual expression of each miR in the cluster indicates that the three miRs contribute equally to anchorage independence, whereas miR-25 has a more significant role in the drug resistance. This suggests that, in addition to EP300, other as yet unidentified miR targets contribute to this phenotype.

In conclusion, we report a novel regulatory axis linking drug resistance, EMT and CSC, which is TGF-β independent. The axis is controlled by the miR-106b ~ 25 cluster via targeting of EP300, a transcriptional activator of E-cadherin, and highlights the plasticity of the cancer cell to activate an aggressive phenotype.

Materials and Methods

Cells. Drug resistance derivatives of pretumorigenic human embryonic skin fibroblasts have been described.[5] MTMEC cells were a gift from William Hahn (Dana Farber, Boston, MA, USA). These cells express TERT, SV40 large T antigen, a constitutively active form of PI3K, p110α and oncogenic RAS and have been previously described.[29] MTMEC cells were routinely cultivated on serum-free HuMEC medium (Life Technologies, Paisley, UK). Doxorubicin-resistant derivatives of MTMEC cells were generated by treating cells with 30 ng/ml doxorubicin for 24 h and then cultured in drug-free medium for three successive passages before treating them with drug again. This process was repeated until cells were able to proliferate after doxorubicin treatment (approximately 10 treatments) and generate MD30 cells. MD60 cells were generated from MD30 cells by exposure to 60 ng/ml doxorubicin in the same manner. HEK293T cells (American Type Culture Collection, LGC Standards, Teddington, UK) were maintained in DMEM supplemented with 4.5 g/l glucose, 10% fetal calf serum and 4 mM L-glutamine (Life Technologies). MCF-7 cells were freshly obtained for this study from Sigma (St. Louis, MO, USA) and were maintained as HEK293T cells.

DNA procedures. An approximately 1-kbp DNA fragment corresponding to intron 13 of *MCM7*, and carrying the miR-106b ~ 25 cluster, was generated by PCR from human genomic DNA using the primers BamHI-106b ~ 25 F and EcoRI -106b ~ 25 R and cloned into pCR2.1-TOPO (Life Technologies). A list of oligonucleotide sequences is shown in Supplementary Table S1. After digestion with *BamH*I and *Eco*RI, the fragment was directionally cloned in *BamH*I- and *Eco*RI-digested lentiviral vector FUW. A similar strategy was used to clone genomic fragments carrying individual miR precursors using primers BamHI-106b ~ 25 F and OLEY382 for miR-106b, OLEY384 and OLEY383 for miR-93 and OLEY385 and EcoRI -106b ~ 25 R for miR-25. A commercial plasmid (SC128224) was obtained from Origene (Rockville, MD, USA) and used to amplify and clone the *MCM7* cDNA into FUW. A commercial lentivector was used to knock-down expression of the miR-106b ~ 25 cluster using miR-Zips (System Biosciences, Mountain View, CA, USA). Downregulation of *EP300* and *CDH1* was obtained by stable expression of hairpins; for *EP300* (clone TRCN0000009883; The RNAi Consortium, Broad Institute, Cambridge, MA, USA) in the pLKO lentiviral vector; for *CDH1* (clone RHS4430-99158891; Open Biosystems, Waltham, MA, USA) in the lentiviral vector pGIPZ. A firefly luciferase reporter with the 3′-UTR of *EP300* cloned in pMirTarget was obtained from Origene. The EP300 target sequence of mir-25 seed (5′-TGCAAT-3′) was mutagenized (5′-TAGACT-3′) by Takara Biotechnology (Dalian, China) and that of miR-196b/93 (5′-CACTTT-3′) was mutagenized (5′-AAAGGT-3′) by Mutagenex (Piscataway, NJ, USA).

Cell transfection. Viral transductions were essentially as described.[56] MTMEC cells and its derivatives were transiently co-transfected with 2 μg EP300 3′-UTR firefly luciferase reporter vector and 50 ng phRGTK (expressing *Renilla* luciferase to normalize for transfection efficiency; Promega, Madison, WI, USA) using an Amaxa HMEC Nucleofector kit (Lonza, Basel, Switzerland) following the manufacturer's recommendations. A Dual-Luciferase reporter assay (Promega) was used to measure both firefly and *Renilla* luciferase 48 h after transfection.

Antibodies. Antibodies for immunodetection following standard immunoblotting procedures were D21H3 for vimentin and 24E10 for E-cadherin (Cell Signalling Technology, Danvers, MA, USA), RW128 for EP300 (Merck Millipore, Billerica, MA, USA), TUB 2.1 for tubulin (Sigma) and C-20 for lamin B (Santa Cruz Biotechnology, Dallas, TX, USA). Appropriate horseradish peroxidase-conjugated secondary antibodies (Cell Signalling

Figure 7 Downregulation of *EP300* or *CDH1* leads to doxorubicin resistance and a phenotype characteristic of EMT. MTMEC cells were stably transfected to express small hairpins targeting *EP300* and *CDH1*. (**a**) Knock-down efficiency was monitored by reverse transcription and real time PCR (upper panels) and immunoblotting (lower panels). (**b**) Downregulation of *EP300* or *CDH1* increases the motility and invasion of MTMEC cells. Upper panels, wound-healing assay; lower panel, solubilization of crystal violet to quantify cells in the transwells with (invasion) or without (migration) Matrigel (left panels). (**c** and **d**) Downregulation of *EP300* or *CDH1* bypasses doxorubicin-induced senescence and enables the generation of proliferating, doxorubicin-resistant clones. (**c**) Cells were treated with 60 ng/ml doxorubicin for 24 h and cells stained for SA-β-galactosidase 3 weeks after. (**d**) Cells were treated for 24 h with 60 ng/ml doxorubicin and drug-resistant clones were stained with crystal violet after 3 weeks (left panels) and counted (right panels). (**e**) Cells were treated with doxorubicin as above and 3 weeks later, trypsinized and seeded (10 000 cells per well in a 96-well plate). Percentage of cells incorporating EdU by fluorescence microscopy (left panels) and EdU incorporation determined by fluorescence detection (right panel). (**f**) Anchorage independence was determined by the formation of clones in soft agar after 4 weeks. Numerical data represent the average ± S.D. of at least three different experiments (*$P < 0.05$). Pictorial data were repeated at least in triplicate and a representative picture is shown

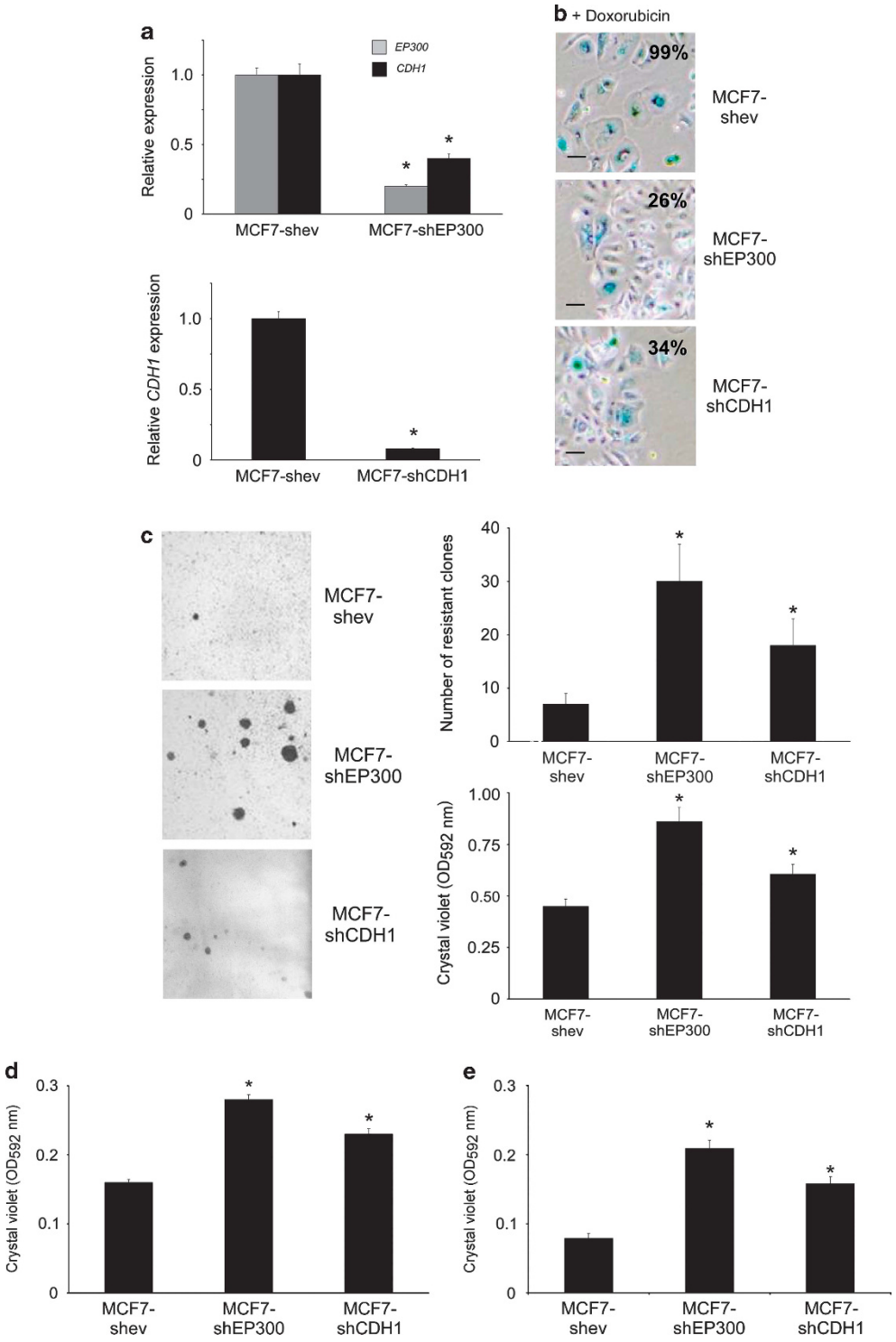

Figure 8 Downregulation of *EP300* or *CDH1* leads to drug resistance and an aggressive phenotype in MCF-7 cells. MCF-7 cells were stably transfected to express small hairpins targeting *EP300* or *CDH1*. (**a**) Knock-down efficiency was monitored by reverse transcription and real time PCR. (**b** and **c**) Downregulation of *EP300* or *CDH1* bypasses doxorubicin-induced senescence and enables the generation of proliferating, doxorubicin-resistant clones. (**b**) Cells were treated with 60 ng/ml doxorubicin for 1 week and cells stained for SA-β-galactosidase 3 weeks after. (**c**) Cells were treated for 1 week with 60 ng/ml doxorubicin and drug-resistant clones were stained with crystal violet after 3 weeks (left panels) and counted (right panels). Down-regulation of *EP300* or *CDH1* increases the motility (**d**) and invasion (**e**) of MCF-7 cells. Crystal violet staining of cells through transwells with (**e**, invasion) or without (**d**, migration) Matrigel. Numerical data represent the average ± S.D. of at least three different experiments (*$P<0.05$). Pictorial data were repeated at least in triplicate and a representative picture is shown

Technology) were detected by enhanced chemiluminescence (GE Healthcare Life Sciences, Pittsburgh, PA, USA).

Anchorage-independent growth assay. Cells (2×10^5) were seeded in 0.3% agar noble in serum-free HuMEC medium on 30-mm plates with a bottom layer of solidified 0.6% agar noble in the same medium. Triplicate cultures for each cell type were maintained for 3 weeks at 37 °C in an atmosphere of 5% CO_2 and 95% air, with 200 μl fresh medium added after 1 week. Colonies of >25 μm in diameter were counted after 3 weeks and stained with crystal violet.

Gene expression analysis. For mRNA detection, total RNA (isolated using a miRCURY RNA isolation kit, Exiqon, Vedbaek, Denmark) was reverse transcribed with RNase H^+ MMLV reverse transcriptase (iScript cDNA synthesis kit, Bio-Rad, Hercules, CA, USA) and real-time quantitative PCR was performed using SYBR-Green (Bioline, London, UK) on an ABI Prism 7700 detection system (PerkinElmer Life Sciences, Waltham, MA, USA). *RPS14* mRNA was used as a normalizer. For miR detection, total RNA was reverse transcribed with TaqMan MicroRNA Reverse Transcription kit and real-time quantitative PCR was performed using TaqMan miR and *U6* RNA (used as a normalizer) assays (Life Technologies) following the manufacturer's instructions. A comparative threshold cycle was used to determine the relative gene expression as previously described.[57] Oligonucleotides used for gene expression analysis are shown in Supplementary Table S1. A customary miR expression profiling using a miRCURY LNA Array version 5th Generation containing all human miRs in the miRBASE version 15.0 was performed by Exiqon.

Flow cytometry. For cell cycle analysis, cells were stained with propidium iodide after fixation with ice-cold 70% methanol and the DNA content determined by flow cytometry essentially as described.[58] For stem cell markers, CD44 (FITC) and CD24 (PE), both form BD Biosciences (San Jose, CA, USA), were used essentially as described.[59]

ALDH activity. An Aldefluor assay kit (StemCell Technologies, Manchester, UK) was used for the determination of ALDH activity by flow cytometry essentially as described.[59] Briefly, cells were resuspended in assay buffer (10^6 cells/ml). Activated Aldefluor substrate (5 μl) was added to samples and incubated at 37 °C for 45 min to allow substrate conversion. A sample with the ALDH inhibitor diethylaminobenzaldehyde was used as a negative control.

Therapy resistance clonogenic assay. MTMEC-derived cells were seeded, at least in duplicate, at a density of 3×10^5 cells in 25-cm^2 culture flasks and exposed to a single dose of doxorubicin (60 ng/ml for MTMEC and 240 ng/ml for drug-resistant MD60 cells) for 24 h. For MCF7 cells, which are intrinsically more resistant to doxorubicin than MTMEC cells, drug treatment was extended for 1 week. Cells were cultured for 21 days with drug-free medium changed every 3 days. Where indicated, cells were irradiated at room temperature with γ-rays (9 Gy at a rate of 0.31 Gy/min) using an IBL-637 irradiator (CIS-Biointernational, Gif Sur Yvette, France) and cultured for 21 days as above. Resistant clones were fixed with 4% paraformaldehyde and stained with 0.2% crystal violet and counted. Crystal violet retained in the cells was quantified by solubilization with 0.5% acetic acid and measurement at OD_{592} nm.

SA β-galactosidase. Cells (1×10^5) were seeded, at least in triplicate, in six-well dishes and treated with doxorubicin for 24 h or exposed to γ-irradiation (9 Gy). After medium replacement, cells were kept in culture until stained for acidic β-galactoside (Cell Signalling Technology), essentially as previously described.[5]

Cell proliferation. Cells (1×10^4) were plated in 96-well dishes and incubated with 10 μM EdU (5-ethynyl-2′-deoxyuridine) for 18 h to allow incorporation into newly synthesized DNA. Detection of the incorporated EdU with the Oregon Green 488 azide was performed with a Click-iT EdU Microplate Assay (Life Technologies) following the manufacturer's recommendations.

Migration and invasion assays. A qualitative wound-healing assay was performed to monitor cell motility after 18 h essentially as described.[60] Transwell migration and invasion assays were performed essentially as described.[59] For MTMEC cells and its derivatives, 5×10^4 cells were seeded in a Matrigel (BD Biosciences)-coated transwell chamber (Corning, Tewksbury, MA, USA) in serum-free HuMEC medium (Life Technologies). After 72 h, cells attached to the under surface of the membrane were fixed with 75% ethanol and stained with 0.1% crystal violet. For migration assays, Matrigel was omitted. For MCF-7 cells, cells were starved in serum-free DMEM medium 24 h before harvesting. To test invasive capacity, 5×10^4 cells were seeded in the top chamber with Matrigel (1 : 20)-coated in serum-free DMEM. DMEM with 20% fetal calf serum was used in the wells that held the chambers. After 72 h, cells were stained with crystal violet.

Statistical analysis. Statistical evaluations were performed by Student's *t*-test for paired data, and data were considered significant at a *P*-value inferior to 0.05.

Conflict of Interest

The authors declare no conflict of interest.

Acknowledgements. We thank William Hahn (Dana Farber, Boston) for a generous gift of human MTMECs and Emanuele de Rinaldis (King's College London) for bioinformatic analyses. This work was supported by Cancer Research UK (to EY and RCC), the Chinese National Natural Sciences Foundation (81170512 to YZ), China Scholarship Council (YH). YZ was the recipient of a Cancer Research UK China Fellowship.

1. Gottesman MM, Fojo T, Bates SE. Multidrug resistance in cancer: role of ATP-dependent transporters. *Nat Rev Cancer* 2002; **2**: 48–58.
2. Raguz S, Yagüe E. Resistance to chemotherapy: new treatments and novel insights into an old problem. *Br J Cancer* 2008; **99**: 387–391.
3. Szakacs G, Paterson JK, Ludwig JA, Booth-Genthe C, Gottesman MM. Targeting multidrug resistance in cancer. *Nat Rev Drug Discov* 2006; **5**: 219–234.
4. Singh A, Settleman J. EMT, cancer stem cells and drug resistance: an emerging axis of evil in the war on cancer. *Oncogene* 2010; **29**: 4741–4751.
5. Yagüe E, Arance A, Kubitza L, O'Hare M, Jat P, Ogilvie CM *et al.* Ability to acquire drug resistance arises early during the tumorigenesis process. *Cancer Res* 2007; **67**: 1130–1137.
6. Minchinton AI, Tannock IF. Drug penetration in solid tumours. *Nat Rev Cancer* 2006; **6**: 583–592.
7. Ewald JA, Desotelle JA, Wilding G, Jarrard DF. Therapy-induced senescence in cancer. *J Natl Cancer Inst* 2010; **102**: 1536–1546.
8. Sliwinska MA, Mosieniak G, Wolanin K, Babik A, Piwocka K, Magalska A *et al.* Induction of senescence with doxorubicin leads to increased genomic instability of HCT116 cells. *Mechanisms Ageing Dev* 2009; **130**: 24–32.
9. Kuilman T, Michaloglou C, Mooi WJ, Peeper DS. The essence of senescence. *Genes Dev* 2010; **24**: 2463–2479.
10. Chang BD, Broude EV, Dokmanovic M, Zhu H, Ruth A, Xuan Y *et al.* A senescence-like phenotype distinguishes tumor cells that undergo terminal proliferation arrest after exposure to anticancer agents. *Cancer Res* 1999; **59**: 3761–3767.
11. Chang BD, Xuan Y, Broude EV, Zhu H, Schott B, Fang J *et al.* Role of p53 and p21waf1/cip1 in senescence-like terminal proliferation arrest induced in human tumor cells by chemotherapeutic drugs. *Oncogene* 1999; **18**: 4808–4818.
12. Jones KR, Elmore LW, Jackson-Cook C, Demasters G, Povirk LF, Holt SE *et al.* p53-Dependent accelerated senescence induced by ionizing radiation in breast tumour cells. *Int J Radiat Biol* 2005; **81**: 445–458.
13. Chicas A, Wang X, Zhang C, McCurrach M, Zhao Z, Mert O *et al.* Dissecting the unique role of the retinoblastoma tumor suppressor during cellular senescence. *Cancer Cell* 2010; **17**: 376–387.
14. Elmore LW, Rehder CW, Di X, McChesney PA, Jackson-Cook CK, Gewirtz DA *et al.* Adriamycin-induced senescence in breast tumor cells involves functional p53 and telomere dysfunction. *J Biol Chem* 2002; **277**: 35509–35515.
15. Elmore LW, Di X, Dumur C, Holt SE, Gewirtz DA. Evasion of a single-step, chemotherapy-induced senescence in breast cancer cells: implications for treatment response. *Clin Cancer Res* 2005; **11**: 2637–2643.
16. Reinhart BJ, Slack FJ, Basson M, Pasquinelli AE, Bettinger JC, Rougvie AE *et al.* The 21-nucleotide let-7 RNA regulates developmental timing in Caenorhabditis elegans. *Nature* 2000; **403**: 901–906.
17. Calin GA, Dumitru CD, Shimizu M, Bichi R, Zupo S, Noch E *et al.* Frequent deletions and down-regulation of micro- RNA genes miR15 and miR16 at 13q14 in chronic lymphocytic leukemia. *Proc Natl Acad Sci USA* 2002; **99**: 15524–15529.
18. Jang JS, Jeon HS, Sun Z, Aubry MC, Tang H, Park CH *et al.* Increased miR-708 expression in NSCLC and its association with poor survival in lung adenocarcinoma from never smokers. *Clin Cancer Res* 2012; **18**: 3658–3667.
19. Calin GA, Sevignani C, Dumitru CD, Hyslop T, Noch E, Yendamuri S *et al.* Human microRNA genes are frequently located at fragile sites and genomic regions involved in cancers. *Proc Natl Acad Sci USA* 2004; **101**: 2999–3004.

20. He L, Thomson JM, Hemann MT, Hernando-Monge E, Mu D, Goodson S *et al.* A microRNA polycistron as a potential human oncogene. *Nature* 2005; **435**: 828–833.
21. Bonci D, Coppola V, Musumeci M, Addario A, Giuffrida R, Memeo L *et al.* The miR-15a-miR-16-1 cluster controls prostate cancer by targeting multiple oncogenic activities. *Nat Med* 2008; **14**: 1271–1277.
22. Yang H, Kong W, He L, Zhao JJ, O'Donnell JD, Wang J *et al.* MicroRNA expression profiling in human ovarian cancer: miR-214 induces cell survival and cisplatin resistance by targeting PTEN. *Cancer Res* 2008; **68**: 425–433.
23. Zhou M, Liu Z, Zhao Y, Ding Y, Liu H, Xi Y *et al.* MicroRNA-125b confers the resistance of breast cancer cells to paclitaxel through suppression of pro-apoptotic Bcl-2 antagonist killer 1 (Bak1) expression. *J Biol Chem* 2010; **285**: 21496–21507.
24. Fang L, Deng Z, Shatseva T, Yang J, Peng C, Du WW *et al.* MicroRNA miR-93 promotes tumor growth and angiogenesis by targeting integrin-beta8. *Oncogene* 2011; **30**: 806–821.
25. Ivanovska I, Ball AS, Diaz RL, Magnus JF, Kibukawa M, Schelter JM *et al.* MicroRNAs in the miR-106b family regulate p21/CDKN1A and promote cell cycle progression. *Mol Cell Biol* 2008; **28**: 2167–2174.
26. Poliseno L, Salmena L, Riccardi L, Fornari A, Song MS, Hobbs RM *et al.* Identification of the miR-106b ~ 25 microRNA cluster as a proto-oncogenic PTEN-targeting intron that cooperates with its host gene MCM7 in transformation. *Sci Signal* 2010; **3**: ra29.
27. Petrocca F, Visone R, Onelli MR, Shah MH, Nicoloso MS, de Martino I *et al.* E2F1-regulated microRNAs impair TGF[beta]-dependent cell-cycle arrest and apoptosis in gastric cancer. *Cancer Cell* 2008; **13**: 272–286.
28. Smith AL, Iwanaga R, Drasin DJ, Micalizzi DS, Vartuli RL, Tan AC *et al.* The miR-106b-25 cluster targets Smad7, activates TGF-beta signaling, and induces EMT and tumor initiating cell characteristics downstream of Six1 in human breast cancer. *Oncogene* 2012; **31**: 5162–5171.
29. Zhao JJ, Gjoerup OV, Subramanian RR, Cheng Y, Chen W, Roberts TM *et al.* Human mammary epithelial cell transformation through the activation of phosphatidylinositol 3-kinase. *Cancer Cell* 2003; **3**: 483–495.
30. Agarwal R, Kaye SB. Ovarian cancer: strategies for overcoming resistance to chemotherapy. *Nat Rev Cancer* 2003; **3**: 502–516.
31. Khongkow M, Olmos Y, Gong C, Gomes AR, Monteiro LJ, Yagüe E *et al.* SIRT6 modulates paclitaxel and epirubicin resistance and survival in breast cancer. *Carcinogenesis* 2013; **34**: 1476–1486.
32. Barpe DR, Rosa DD, Froehlich PE. Pharmacokinetic evaluation of doxorubicin plasma levels in normal and overweight patients with breast cancer and simulation of dose adjustment by different indexes of body mass. *Eur J Pharm Sci* 2010; **41**: 458–463.
33. Shi YK, Yu YP, Tseng GC, Luo JH. Inhibition of prostate cancer growth and metastasis using small interference RNA specific for minichromosome complex maintenance component 7. *Cancer Gene Ther* 2010; **17**: 694–699.
34. Wang J, Tai LS, Tzang CH, Fong WF, Guan XY, Yang M. 1p31, 7q21 and 18q21 chromosomal aberrations and candidate genes in acquired vinblastine resistance of human cervical carcinoma KB cells. *Oncol Rep* 2008; **19**: 1155–1164.
35. Dean M, Fojo T, Bates S. Tumour stem cells and drug resistance. *Nat Rev Cancer* 2005; **5**: 275–284.
36. Morel AP, Lievre M, Thomas C, Hinkal G, Ansieau S, Puisieux A. Generation of breast cancer stem cells through epithelial-mesenchymal transition. *PLoS One* 2008; **3**: e2888.
37. Awad O, Yustein JT, Shah P, Gul N, Katuri V, O'Neill A *et al.* High ALDH activity identifies chemotherapy-resistant Ewing's sarcoma stem cells that retain sensitivity to EWS-FLI1 inhibition. *PLoS One* 2010; **5**: e13943.
38. Liang Y, McDonnell S, Clynes M. Examining the relationship between cancer invasion/metastasis and drug resistance. *Curr Cancer Drug Targets* 2002; **2**: 257–277.
39. Betel D, Wilson M, Gabow A, Marks DS, Sander C. The microRNA.org resource: targets and expression. *Nucleic Acids Res* 2008; **36**(Database issue): D149–D153.
40. Liu YN, Lee WW, Wang CY, Chao TH, Chen Y, Chen JH. Regulatory mechanisms controlling human E-cadherin gene expression. *Oncogene* 2005; **24**: 8277–8290.
41. Gal A, Sjoblom T, Fedorova L, Imreh S, Beug H, Moustakas A. Sustained TGF beta exposure suppresses Smad and non-Smad signalling in mammary epithelial cells, leading to EMT and inhibition of growth arrest and apoptosis. *Oncogene* 2008; **27**: 1218–1230.
42. Zubeldia IG, Bleau AM, Redrado M, Serrano D, Agliano A, Gil-Puig C *et al.* Epithelial to mesenchymal transition and cancer stem cell phenotypes leading to liver metastasis are abrogated by the novel TGFbeta1-targeting peptides P17 and P144. *Exp Cell Res* 2013; **319**: 12–22.
43. Bryan EJ, Jokubaitis VJ, Chamberlain NL, Baxter SW, Dawson E, Choong DY *et al.* Mutation analysis of EP300 in colon, breast and ovarian carcinomas. *Int J Cancer* 2002; **102**: 137–141.
44. Gayther SA, Batley SJ, Linger L, Bannister A, Thorpe K, Chin SF *et al.* Mutations truncating the EP300 acetylase in human cancers. *Nat Genet* 2000; **24**: 300–303.
45. Krubasik D, Iyer NG, English WR, Ahmed AA, Vias M, Roskelley C *et al.* Absence of p300 induces cellular phenotypic changes characteristic of epithelial to mesenchyme transition. *Br J Cancer* 2006; **94**: 1326–1332.
46. Li Y, VandenBoom TG 2nd, Kong D, Wang Z, Ali S, Philip PA *et al.* Up-regulation of miR-200 and let-7 by natural agents leads to the reversal of epithelial-to-mesenchymal transition in gemcitabine-resistant pancreatic cancer cells. *Cancer Res* 2009; **69**: 6704–6712.
47. Ma L, Young J, Prabhala H, Pan E, Mestdagh P, Muth D *et al.* miR-9, a MYC/MYCN-activated microRNA, regulates E-cadherin and cancer metastasis. *Nat Cell Biol* 2010; **12**: 247–256.
48. Miller TE, Ghoshal K, Ramaswamy B, Roy S, Datta J, Shapiro CL *et al.* MicroRNA-221/222 confers tamoxifen resistance in breast cancer by targeting p27Kip1. *J Biol Chem* 2008; **283**: 29897–29903.
49. Xu CX, Xu M, Tan L, Yang H, Permuth-Wey J, Kruk PA *et al.* MicroRNA miR-214 regulates ovarian cancer cell stemness by targeting p53/Nanog. *J Biol Chem* 2012; **287**: 34970–34978.
50. Hudson RS, Yi M, Esposito D, Glynn SA, Starks AM, Yang Y *et al.* MicroRNA-106b-25 cluster expression is associated with early disease recurrence and targets caspase-7 and focal adhesion in human prostate cancer. *Oncogene* 2013; **32**: 4139–4147.
51. Blenkiron C, Goldstein LD, Thorne NP, Spiteri I, Chin SF, Dunning MJ *et al.* MicroRNA expression profiling of human breast cancer identifies new markers of tumor subtype. *Genome Biol* 2007; **8**: R214.
52. Derksen PW, Liu X, Saridin F, van der Gulden H, Zevenhoven J, Evers B *et al.* Somatic inactivation of E-cadherin and p53 in mice leads to metastatic lobular mammary carcinoma through induction of anoikis resistance and angiogenesis. *Cancer Cell* 2006; **10**: 437–449.
53. Onder TT, Gupta PB, Mani SA, Yang J, Lander ES, Weinberg RA. Loss of E-cadherin promotes metastasis *via* multiple downstream transcriptional pathways. *Cancer Res* 2008; **68**: 3645–3654.
54. Zhou S, Schuetz JD, Bunting KD, Colapietro AM, Sampath J, Morris JJ *et al.* The ABC transporter Bcrp1/ABCG2 is expressed in a wide variety of stem cells and is a molecular determinant of the side-population phenotype. *Nat Med* 2001; **7**: 1028–1034.
55. Shafee N, Smith CR, Wei S, Kim Y, Mills GB, Hortobagyi GN *et al.* Cancer stem cells contribute to cisplatin resistance in Brca1/p53-mediated mouse mammary tumors. *Cancer Res* 2008; **68**: 3243–3250.
56. Raguz S, Adams C, Masrour N, Rasul S, Papoutsoglou P, Hu Y *et al.* Loss of O(6)-methylguanine-DNA methyltransferase confers collateral sensitivity to carmustine in topoisomerase II-mediated doxorubicin resistant triple negative breast cancer cells. *Biochem Pharmacol* 2013; **85**: 186–196.
57. Yagüe E, Armesilla AL, Harrison G, Elliott J, Sardini A, Higgins CF *et al.* P-glycoprotein (MDR1) expression in leukemic cells is regulated at two distinct steps, mRNA stabilization and translational initiation. *J Biol Chem* 2003; **278**: 10344–10352.
58. Rasul S, Balasubramanian R, Filipovic A, Slade MJ, Yagüe E, Coombes RC. Inhibition of gamma-secretase induces G2/M arrest and triggers apoptosis in breast cancer cells. *Br J Cancer* 2009; **100**: 1879–1888.
59. Lombardo Y, Filipovic A, Molyneux G, Periyasamy M, Giamas G, Hu Y *et al.* Nicastrin regulates breast cancer stem cell properties and tumor growth *in vitro* and *in vivo*. *Proc Natl Acad Sci USA* 2012; **109**: 16558–16563.
60. Liang C-C, Park AY, Guan J-L. *In vitro* scratch assay: a convenient and inexpensive method for analysis of cell migration *in vitro*. *Nat Protocols* 2007; **2**: 329–333.

Supplementary Information accompanies this paper on Cell Death and Differentiation website (http://www.nature.com/cdd)